

# Antituberculosis thiophenes define a requirement for Pks13 in mycolic acid biosynthesis

Regina Wilson<sup>1-3,11</sup>, Pradeep Kumar<sup>1-3,11</sup>, Vijay Parashar<sup>4</sup>, Catherine Vilchèze<sup>5,6</sup>, Romain Veyron-Churlet<sup>7,12</sup>, Joel S Freundlich<sup>2,3,8</sup>, S Whitney Barnes<sup>9</sup>, John R Walker<sup>9</sup>, Michael J Szymonifka<sup>2,3,8</sup>, Emily Marchiano<sup>1-3</sup>, Shubhada Shenai<sup>1-3</sup>, Roberto Colangeli<sup>1-3</sup>, William R Jacobs Jr<sup>5,6</sup>, Matthew B Neiditch<sup>4</sup>, Laurent Kremer<sup>7,10</sup> & David Alland<sup>1-3\*</sup>

**We report a new class of thiophene (TP) compounds that kill *Mycobacterium tuberculosis* by the previously uncharacterized mechanism of Pks13 inhibition. An F79S mutation near the catalytic Ser55 site in Pks13 conferred TP resistance in *M. tuberculosis*. Overexpression of wild-type Pks13 resulted in TP resistance, and overexpression of the Pks13<sup>F79S</sup> mutant conferred high resistance. *In vitro*, TP inhibited fatty acyl-AMP loading onto Pks13. TP inhibited mycolic acid biosynthesis in wild-type *M. tuberculosis*, but it did so to a much lesser extent in TP-resistant *M. tuberculosis*. TP treatment was bactericidal and equivalent to treatment with the first-line drug isoniazid, but it was less likely to permit emergent resistance. Combined isoniazid and TP treatment resulted in sterilizing activity. Computational docking identified a possible TP-binding groove within the Pks13 acyl carrier protein domain. This study confirms that *M. tuberculosis* Pks13 is required for mycolic acid biosynthesis, validates it as a druggable target and demonstrates the therapeutic potential of simultaneously inhibiting multiple targets in the same biosynthetic pathway.**

The emergence of drug-resistant *M. tuberculosis* is rapidly becoming a major global health concern<sup>1,2</sup>. The current pace of drug development is too slow to meet the clinical requirement for new antituberculosis agents. Despite identification of several essential genes and pathways<sup>3</sup>, along with substantial progress in the understanding of *M. tuberculosis* biochemistry and metabolism, few new drug targets have been validated. It is a well-known fact that not all essential metabolic processes represent good drug targets whose inhibition leads to cell death and a therapeutic effect<sup>4-6</sup>. However, decades of drug development have proven that the bacterial cell wall is a rich source of druggable targets<sup>7-10</sup>. In the case of *M. tuberculosis*, isoniazid (INH), ethambutol (EMB) and ethionamide all inhibit cell wall biosynthesis.

Mycolic acids are essential components of the mycobacterial cell wall. They are critical for the pathogenesis of *M. tuberculosis* and have been shown to be important in virulence and persistence *in vivo*<sup>11-13</sup>. Mycolic acids are C<sub>60</sub>-C<sub>90</sub> branched-chain  $\beta$ -hydroxylated fatty acids that are covalently bound to arabinogalactan-peptidoglycan, forming the mycolyl-arabinogalactan peptidoglycan complex<sup>14</sup>. They are also found noncovalently associated to the outer membrane as trehalose monomycolates (TMMs) and trehalose dimycolates (TDMs)<sup>15-17</sup> or as free lipids in mycobacterial biofilms<sup>18</sup>. Pks13 has a critical role in mycolic acid biosynthesis in *M. tuberculosis*<sup>19,20</sup>; it joins the  $\alpha$ -alkyl C<sub>26</sub> fatty acid branch (originating from fatty acid synthase I (FAS-I)) and the meromycolic acid

(C<sub>48</sub>-C<sub>64</sub>)<sup>13</sup> branch (originating from FAS-II) activated by FadD32 (ref. 21) through a Claisen-type condensation reaction to form  $\alpha$ -alkyl  $\beta$ -ketoacids. Pks13 belongs to the type I polyketide synthase gene family and is essential for survival of *Mycobacterium smegmatis* but not for *Corynebacterium glutamicum*<sup>20</sup>. *M. tuberculosis* Pks13 contains acyl carrier protein (ACP) domains located at the N terminus (N-ACP) and C terminus (C-ACP), a ketoacyl synthase, an acyl transferase and a thioesterase domain<sup>19,20</sup>. The N- and C-ACP domains contain 4'-phosphopantetheine attachment (P-pant) sites at Ser55 and Ser1266, respectively. For Pks13 to perform a condensation reaction, a meromycolic acid is converted to a meromycoloyl-AMP and loaded onto the P-pant-binding site at the N-ACP of Pks13 by FadD32, a fatty acyl-AMP ligase<sup>21</sup>. The meromycoloyl-AMP is then transferred to the ketoacyl synthase domain, and Pks13 completes the condensation reaction in a series of steps outlined in **Supplementary Results, Supplementary Figure 1** (ref. 19).

Although the role of Pks13 has not been confirmed *in vivo* in *M. tuberculosis*, an activated recombinant *M. tuberculosis* Pks13 can catalyze fatty acid chain-condensing activity *in vitro*<sup>19</sup>, and the *M. tuberculosis* operon containing the *accD4*, *pks13* and *fadD32* genes is essential<sup>20,22,23</sup>. Herein, we identified and investigated the mechanism of action of a new class of TP compounds with whole-cell activity against *M. tuberculosis* and determined that they act by selectively inhibiting Pks13. Two inhibitors of this class were used to decipher the microbiological and biochemical consequences of

<sup>1</sup>Division of Infectious Disease, New Jersey Medical School, University of Medicine and Dentistry of New Jersey, Newark, New Jersey, USA. <sup>2</sup>Department of Medicine, New Jersey Medical School, University of Medicine and Dentistry of New Jersey, Newark, New Jersey, USA. <sup>3</sup>Ruy V. Lourenco Center for the Study of Emerging and Reemerging Pathogens, New Jersey Medical School, University of Medicine and Dentistry of New Jersey, Newark, New Jersey, USA. <sup>4</sup>Department of Microbiology and Molecular Genetics, New Jersey Medical School, University of Medicine and Dentistry of New Jersey, Newark, New Jersey, USA. <sup>5</sup>Department of Microbiology and Immunology, Albert Einstein College of Medicine, Bronx, New York, USA. <sup>6</sup>Howard Hughes Medical Institute, Albert Einstein College of Medicine, Bronx, New York, USA. <sup>7</sup>Laboratoire de Dynamique des Interactions Membranaires Normales et Pathologiques, Centre National de la Recherche Scientifique, Unité Mixte de Recherche 5235, Université de Montpellier 2, Montpellier, France. <sup>8</sup>Department of Pharmacology and Physiology, New Jersey Medical School, University of Medicine and Dentistry of New Jersey, Newark, New Jersey, USA. <sup>9</sup>Genomics Institute of the Novartis Research Foundation, San Diego, California, USA. <sup>10</sup>Institut National de la Santé et de la Recherche Médicale, Dynamique des Interactions Membranaires Normales, Montpellier, France. <sup>11</sup>These authors contributed equally to this work. <sup>12</sup>Present address: Centre d'Infection et Immunité, Institut Pasteur de Lille, Lille, France. \*e-mail: allandda@umdnj.edu

Pks13 inhibition, explore their potential as drug leads and characterize the structural requirements for activity against *M. tuberculosis*.

## RESULTS

### Whole-cell screen for new *M. tuberculosis* cell wall inhibitors

We searched for new inhibitors of mycobacterial cell wall biosynthesis with the goal of identifying new drug targets and new classes of inhibitors with potent activity against *M. tuberculosis*. To search for inhibitors, we screened for compounds that induced expression of the *M. tuberculosis* *iniBAC* operon promoter (*piniBAC*; **Supplementary Table 1**). The *iniBAC* gene cluster is highly induced by a broad range of cell wall biosynthesis inhibitors<sup>24</sup>. We screened a library of 1,113 publically available compounds with known activity against *M. tuberculosis* on a whole-cell basis<sup>25,26</sup>. By interrogating experimental controls, we confirmed that the *piniBAC* screen correctly identified the known *piniBAC* inducers INH (**1**) and EMB (**2**). Compounds that caused a four-fold or greater induction were then selected for further study, resulting in the identification of a number of TP analogs (**Table 1**). Structural analogs of SQ109, another known inducer of *piniBAC*, were also identified<sup>27</sup>. The minimal inhibitory concentration (MIC) values of the TPs against *M. tuberculosis* strain H37Rv ranged from 0.5  $\mu$ M to 20.2  $\mu$ M, with TP2 (**3**) and TP4 (compound **4**) where the number following the TP prefix represents a compound number in the series) being among the most active. The three most potent compounds against *M. tuberculosis* (MIC values 0.5–1.0  $\mu$ M), namely TP2, TP4 and TP626 (**5**), also had the greatest fold inductions of the *iniBAC* reporter (10.1–14.6). Notably, TP2 and TP4 (were equally active against laboratory, clinical drug-susceptible and clinical multidrug-resistant *M. tuberculosis* strains (**Table 2**). All of the nontuberculous mycobacteria tested were highly resistant to TP2, including *M. smegmatis* (**Supplementary Table 2**). Structure-activity relationship (SAR) analysis indicated that replacement of the pentafluorophenyl amide in these most potent hits with a 2-fluorophenylamide or 4-methylphenylamide (TP2 to compound **6**, TP175 or compound **7**, TP197) resulted in substantial losses of activity (**Table 1**). Exchanging the 3-alkyl ester for a primary amide (TP2 to compound **8**, TP953) or carboxylic acid (TP4 to compound **9**, TP1735) and transposition of the 3-ester and 5-amide functionalities (TP4 to compound **10**, TP238) also caused a substantial loss of whole-cell activity.

### Isolation of resistant mutants and whole-genome sequencing

*M. tuberculosis* cultures ( $10^7$  cells) were plated on solid agar containing 4 $\times$  and 8 $\times$  the MIC of TP2 or TP4. One mutant (DRM2) obtained on the 4 $\times$  TP2 plate had a four-fold increase in MIC to TP2 in liquid medium (3.8  $\mu$ M) (**Table 2**). DRM2 also had a four-fold increase in MIC to TP4 (1.9  $\mu$ M), indicating an overlapping target with TP2; however, we failed to directly isolate resistant mutants by plating on TP4. Whole-genome sequencing of DRM2 revealed a solitary T236C single-nucleotide polymorphism (SNP) in the *pks13* (also known as *Rv3800c*) gene, which produced a F79S substitution.

### Overexpression of Pks13 increases TP resistance

Overexpressing a gene encoding a drug target is expected to generate an increase in the MIC for that drug<sup>9</sup>. Therefore, to determine whether Pks13 is involved in TP2 and TP4 activity, we overexpressed wild-type *M. tuberculosis* Pks13 in *M. bovis* bacillus Calmette-Guérin (BCG) using two multicopy plasmids expressing Pks13 with either a C terminus (pVV16-*pks13*) or N terminus (pMK1-*pks13*) His<sub>6</sub> tag driven by the *hsp60* promoter. Pks13 expression from pMK1-*pks13* was confirmed (**Supplementary Fig. 2a**). This strain showed a four- to six-fold increase in MIC to both TP2 and TP4 (**Table 2**). Results were similar when Pks13 was expressed from pVV16-*pks13* (**Table 2**). Comparable resistance to TP2 and TP4 was observed in *M. tuberculosis* strain mc<sup>2</sup>7000 carrying pMK1-*pks13* (**Table 2**). We were unable to stably express Pks13 in *M. tuberculosis* H37Rv

or DRM2 from multicopy plasmids. Therefore, we constructed integrative plasmids to express wild-type Pks13 and mutant Pks13 (Pks13<sup>F79S</sup>) under the *hsp60* promoter (H37Rv::pMV306H-*pks13* and H37Rv::pMV306H-*pks13\_F79S*, respectively). The overexpression of Pks13 proteins was verified by SDS-PAGE (**Supplementary Fig. 2b**). Overexpression of wild-type Pks13 in H37Rv resulted in only a two-fold increase in resistance to TP2. However, overexpression of the TP-resistant Pks13<sup>F79S</sup> mutant resulted in very high resistance to TP2 (64  $\mu$ M) in both H37Rv (H37Rv::pMV306H-*pks13\_F79S*) and DRM2 (DRM2::pMV306H-*pks13\_F79S*). These results closely parallel those found in a previous study that validated *embB* as the target of EMB in *M. tuberculosis*<sup>28</sup>. Resistance to TP4 was also increased, although to a lesser degree (four-fold in H37Rv and eight-fold in DRM2). Notably, overexpression of Pks13 failed to increase resistance to unrelated drugs such as INH, EMB, rifampicin (RIF), DA5 (**11**) (a recently identified MmpL3 inhibitor<sup>27</sup>) and cephalexin (**Table 2** and **Supplementary Table 3**), thus highlighting the specificity of the TP inhibitory mechanism.

### TP2 and TP4 inhibit mycolic acid biosynthesis

To test whether treatment with TP2 or TP4 alters mycolic acid synthesis in *M. tuberculosis* through Pks13 inhibition, we treated H37Rv and the TP2-resistant mutant strain (DRM2) with increasing concentrations of either TP2 or TP4 or the antituberculosis drugs INH (a positive control that inhibits mycolic acid biosynthesis) or the DNA gyrase inhibitor ciprofloxacin<sup>29</sup> (a negative control that does not inhibit mycolic acid biosynthesis) before labeling the cultures with [<sup>14</sup>C]acetate. Radiolabeled total lipids were then extracted, methyl esterified and analyzed by TLC autoradiography. Treatment with either TP2 or TP4 at starting concentrations of 0.5 $\times$  MIC produced visible suppression of mycolic acid methyl esters (MAMEs;  $\alpha$ -MAME, methoxy-MAME and keto-MAME) in wild-type *M. tuberculosis*. Complete suppression of mycolic acid synthesis occurred at higher concentrations with concomitant accumulation of fatty acid methyl esters (FAMEs; **Fig. 1a** and **Supplementary Fig. 3a**). In contrast to their effect on H37Rv, neither TP2 nor TP4 showed substantial suppression of mycolic acid biosynthesis in the DRM2 strain, except for TP4 at very high concentrations (125 $\times$  MIC). As expected, mycolic acid synthesis was also inhibited by INH (**Fig. 1b**) but not by ciprofloxacin (**Supplementary Fig. 3b**). The FAMEs from TP-treated cultures were further analyzed by reverse-phase TLC (RP-TLC) (**Fig. 1c,d**). This analysis showed accumulation of all of the fatty acids upon treatment with TP2, including C<sub>16</sub>, C<sub>18</sub> and C<sub>20</sub> fatty acids as well as C<sub>26</sub> fatty acid, a FAS-I end product that is also a Pks13 substrate. The exact chain lengths of the compounds observed on RP-TLC were determined by their comigration (identical R<sub>f</sub> values) with synthetic FAMEs (**Supplementary Fig. 4**). Furthermore, analysis of polar lipids upon treatment with TP2 showed a decline in the amounts of TMM and TDM, similar to the effect of INH and consistent with Pks13 inhibition (**Fig. 1e,f** and **Supplementary Fig. 5**). In contrast, DA5 suppressed only TDM, and EMB resulted in a slight accumulation of both TMM and TDM, as expected<sup>27</sup> (**Fig. 1e,f**). To further confirm the specificity of TPs, we also examined the apolar lipid fraction of H37Rv treated with up to 20 $\times$  the MIC of TP2. A comprehensive analysis of extractable lipids (**Fig. 1e,f** and **Supplementary Fig. 6**) did not reveal a loss of other lipids, such as phthiocerol dimycocerosate or sulfolipid-1. Together with the overexpression results, these findings strongly suggest that the antituberculosis activity of TP2 and TP4 occurs via inhibition of Pks13 and mycolic acid biosynthesis.

### Tps inhibit FadD32-dependent loading onto N-ACP of Pks13

Our observation that the TP-resistant DRM2 strain had a F79S mutation near the essential residue of the Pks13 N-ACP domain suggested that TP compounds act by interfering with this site. We postulated that TP compounds block loading of the meromycoloyl

**Table 1 | Thiophenes: structures, MIC values against *M. tuberculosis* and amount of *piniBAC* induction.**

| Compound  | Structure | MIC ( $\mu\text{M}$ ) | <i>piniBAC</i> fold induction | Compound   | Structure | MIC ( $\mu\text{M}$ ) | <i>piniBAC</i> fold induction |
|-----------|-----------|-----------------------|-------------------------------|------------|-----------|-----------------------|-------------------------------|
| (1) INH   |           | 0.2                   | 11-18                         | (9) TP1735 |           | 78.4                  | ND                            |
| (2) EMB   |           | 7.2                   | 14-39                         | (10) TP238 |           | 4.9                   | 10.1                          |
| (3) TP2   |           | 1.0                   | 14.6                          | (11) DA5   |           | 10                    | 21                            |
| (4) TP4   |           | 0.5                   | 10.8                          | (12) TP506 |           | 2.1                   | 8.6                           |
| (5) TP626 |           | 1.0                   | 10.1                          | (13) TP338 |           | 7.1                   | 8.8                           |
| (6) TP175 |           | 20.2                  | 1.4                           | (14) TP464 |           | 3.5                   | 4.3                           |
| (7) TP197 |           | >20.2                 | ND                            | (15) TP514 |           | 1.9                   | 8.2                           |
| (8) TP953 |           | 15.3                  | 2                             | (16) TP584 |           | 10.6                  | 0.8                           |

Fold induction of *piniBAC* was determined by the  $D_{420\text{ nm}}$  of the reporter strain cultured in the presence of compounds divided by the  $D_{420\text{ nm}}$  the reporter strain cultured without drug. EMB and INH treated cultures were used as positive induction controls. ND, not determined.

**Table 2 | Lead thiophene MIC values of drug-susceptible, drug-resistant and Pks13-overexpressing strains.**

| Strain                          | Drug resistance             | Strain type | TP2 ( $\mu\text{M}$ ) | TP4 ( $\mu\text{M}$ ) | INH ( $\mu\text{M}$ ) |
|---------------------------------|-----------------------------|-------------|-----------------------|-----------------------|-----------------------|
| H37Rv                           | No                          | Lab         | 1.0                   | 0.5                   | 0.2                   |
| 210                             | No                          | Clinical    | 1.0                   | 0.5                   | 0.2                   |
| 692                             | No                          | Clinical    | 1.0                   | 0.5                   | 0.2                   |
| 91                              | RIF, EMB                    | Clinical    | 1.0                   | 0.5                   | 0.4                   |
| 36                              | INH, RIF, EMB               | Clinical    | 1.0                   | 0.9                   | >23.3                 |
| 116                             | INH, EMB, PAS               | Clinical    | 1.0                   | 0.5                   | >23.3                 |
| 31                              | INH, RIF, EMB, KAN, SM, CAP | Clinical    | 1.0                   | 0.5                   | >23.3                 |
| DRM2                            | TP2, TP4                    | Lab         | 3.8                   | 1.9                   | 0.2                   |
| H37Rv- $\Delta katG$            | INH                         | Lab         | 1.0                   | 0.5                   | >1400                 |
| H37Rv-P <sub>mabA inhA</sub>    | INH                         | Lab         | 1.0                   | 0.5                   | 5.8                   |
| H37Rv                           | No                          | Lab         | 2.0                   | 1.0                   | 0.4                   |
| H37Rv::pMV306H                  | HYG                         | Lab         | 2.0                   | 1.0                   | 0.4                   |
| H37Rv::pMV306H-pks13            | HYG                         | Lab         | 4.0                   | 2.0                   | 0.4                   |
| H37Rv::pMV306H-pks13_F79S       | HYG                         | Lab         | 64.0                  | 4.0                   | 0.4                   |
| DRM2                            | TP2, TP4                    | Lab         | 8.0                   | 2.0                   | 0.4                   |
| DRM2::pMV306H                   | HYG                         | Lab         | 8.0                   | 2.0                   | 0.2                   |
| DRM2::pMV306H-pks13             | HYG                         | Lab         | 16.0                  | 2.0                   | 0.4                   |
| DRM2::pMV306H-pks13_F79S        | HYG                         | Lab         | 64.0                  | 8.0                   | 0.4                   |
| mc <sup>2</sup> 7000 pMK1       | KAN                         | Lab         | 1.25                  | 0.6                   | 0.4                   |
| mc <sup>2</sup> 7000 pMK1-pks13 | KAN                         | Lab         | 6.25                  | 6.25                  | 0.2                   |
| BCG pMK1                        | KAN                         | Lab         | 0.6                   | 0.2                   | ND                    |
| BCG pMK1-pks13                  | KAN                         | Lab         | >2.4                  | >1.2                  | ND                    |
| BCG pVV16                       | HYG                         | Lab         | 0.6                   | 0.2                   | ND                    |
| BCG pVV16-pks13                 | HYG                         | Lab         | >1.2                  | >0.6                  | ND                    |

KAN, kanamycin; SM, streptomycin; CAP, capreomycin; PAS, *para*-aminosalicylic acid; HYG, hygromycin; ND, not determined. MIC values for H37Rv  $\Delta katG$  and H37Rv P<sub>mabA inhA</sub> were performed in liquid medium<sup>31</sup>. The MIC values in shaded rows were determined by microdilution in 96-well plates. BCG and mc<sup>2</sup>7000 MIC values were determined by spotting on agar plates. All of the other MIC values were determined by BACTEC.

chain onto the Pks13 N-ACP domain. We purified wild-type Pks13 and Pks13<sup>F79S</sup> by coexpressing the *Bacillus subtilis* *sfp* gene<sup>19</sup> to ensure phosphopantetheinylation at Ser55 (confirmed by nano-LC/MS/MS analysis, which showed a 340-Da increase in mass; **Supplementary Fig. 7**). The N-ACP loading step is FadD32 dependent<sup>21</sup> and has been previously demonstrated using <sup>14</sup>C-labeled C<sub>12</sub> (lauric acid) and C<sub>16</sub> (palmitic acid) fatty acids as substrates<sup>19</sup>. We developed a nonradioactive assay to measure meromycoloyl loading using a fluorescent analog of palmitic acid (BODIPY FL C<sub>16</sub>). The loading of FL C<sub>16</sub> onto Pks13 was specific and FadD32 dependent, as demonstrated by the observations that the negative controls BSA, NS5B (an RNA-dependent RNA polymerase from hepatitis C) and heat-inactivated proteins failed to load FL C<sub>16</sub> onto Pks13. Furthermore, we showed that the phosphopantetheinylation of Pks13 was required for FL C<sub>16</sub> loading (**Supplementary Fig. 8**). We next examined whether the TP compounds inhibited FL C<sub>16</sub> loading onto Pks13. The results showed that TP2 inhibited loading of wild-type Pks13 in a dose-dependent manner (**Fig. 2a**). TP2 also inhibited FL C<sub>16</sub> loading onto the TP-resistant F79S mutant protein (**Fig. 2b**). The difference in the ability of TP2 to inhibit loading of the wild-type Pks13 versus the F79S mutant was modest, but it was most noticeable at equimolar concentrations (1  $\mu\text{M}$ ) of protein and inhibitors. Similar inhibition kinetics were observed with TP4 (**Supplementary Fig. 9a–c**). In contrast, TP1735, which had some of the poorest activity against live *M. tuberculosis*, also failed to inhibit loading on either wild-type Pks13 or Pks13<sup>F79S</sup> (~10% inhibition against wild-type Pks13 and no inhibition against Pks13<sup>F79S</sup>). *M. smegmatis* is highly resistant to the TPs (MIC >128  $\mu\text{M}$ ), and purified *M. smegmatis* Pks13 (MsmPks13) was also highly resistant

to inhibition of FL C<sub>16</sub> loading by TP2 (**Fig. 2c**), although this comparison was best appreciated from the inhibition curves (**Fig. 2d**). We also ruled out any potential direct inhibition of FadD32 activity by TP2 or TP4 (**Supplementary Fig. 10**)<sup>30</sup>. Overall, these data further support our *in vivo* findings that TP compounds specifically and directly target *M. tuberculosis* Pks13.

#### Lack of cross-resistance between the TP compounds and INH

Although INH does not share structural similarities with the TP class of compounds (**Table 1**), INH behaves like the TPs in that it is a strong inducer of *piniBAC* and a potent inhibitor of mycolic acid biosynthesis at the *InhA* step in the FAS-II pathway. We therefore tested for cross-resistance between INH, TP2 and TP4 to confirm that these compounds inhibited different molecular targets. MIC values were determined against H37Rv *katG*<sup>31</sup>, an *M. tuberculosis* strain where deletion of the gene encoding the activator of INH, *katG*, causes it to be deficient in INH activation. MIC values were also determined against H37Rv P<sub>mabA inhA</sub> (mc<sup>2</sup>4914)<sup>9</sup>, an *M. tuberculosis* strain that is INH resistant owing to a promoter-up mutation (c15t) in *inhA*, the gene encoding the INH target. Although each of these mutants was highly resistant to INH, neither of them showed an increase in MIC to TP2 or TP4 (**Table 2**). INH MIC values were also quantified for the TP-resistant mutant DRM2, and no increase in INH MIC was noted relative to wild-type controls (**Table 2**). The lack of cross-resistance between INH-resistant and TP-resistant mutants provides further confirmation that these two compounds involve different mechanisms of action within the mycolic acid biosynthetic pathway: INH targets *InhA*, and TPs target Pks13.

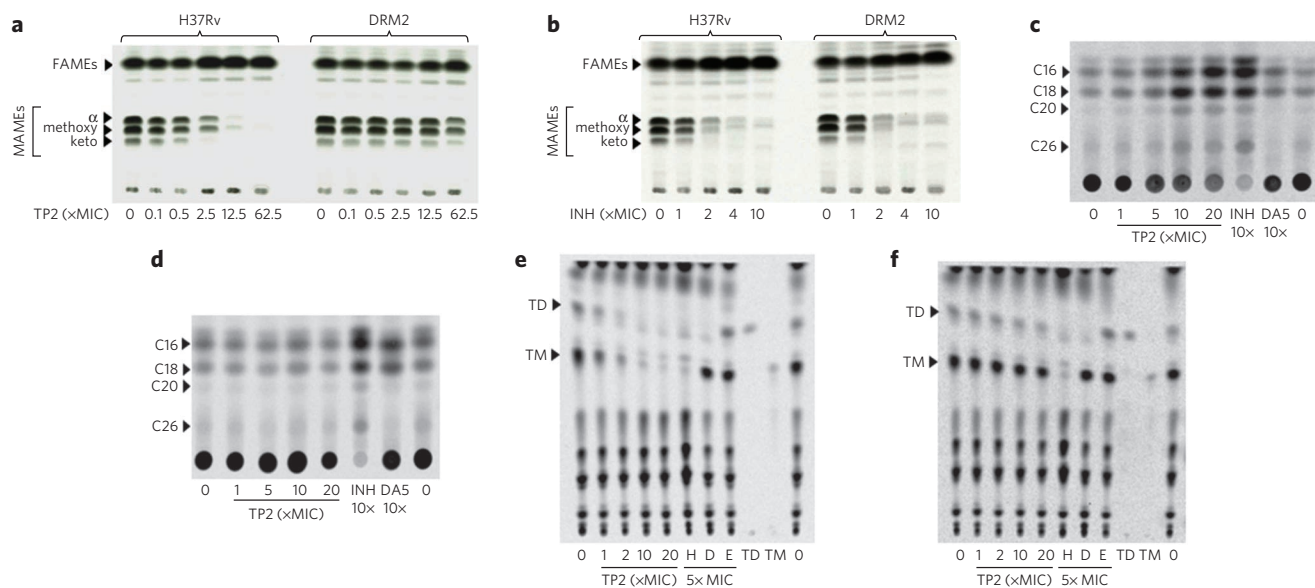


**Figure 1 | Effect of TP2 and TP4 on mycolic acid biosynthesis in *M. tuberculosis*.** (a,b) Normal-phase TLC analysis of MAMES and FAMES from wild-type *M. tuberculosis* (H37Rv) and TP-resistant *M. tuberculosis* (DRM2) after treatment with increasing concentrations of TP2 (a) or INH (b). Equal counts were loaded, and the TLC was developed using hexane/ethyl acetate (19:1, v/v, two runs) solvent system. Similar TLCs upon TP4 or ciprofloxacin treatment are shown in **Supplementary Figure 3**. (c,d) Reverse-phase TLCs using acetonitrile/dioxane solvent (1:1, v/v and equal volumes of samples) showing the fatty acid chain length of the FAS-I-derived products following treatment with TP2, INH or DA5 from H37Rv (c) or DRM2 (d). Cold methyl esters of fatty acids were used as standards as shown in **Supplementary Figure 4**. (e,f) Normal-phase TLCs showing TMM (TM) and TDM (TD) from polar lipids extracted from H37Rv (e) or DRM2 (f) upon treatment with increasing concentrations of TP2 or 5× MIC of INH (H), DA5 (D) or EMB (E). An equal volume (5 μl) of each sample was analyzed on a silica gel 60 F254, which was developed with CHCl<sub>3</sub>/CH<sub>3</sub>OH/H<sub>2</sub>O (62:25:4, v/v/v).

### Combining TP2 or TP4 with INH enhances killing

It is not known whether inhibition of two distinct targets within the same mycolic acid biosynthesis pathway will have synergistic or antagonistic effects. The availability of TP compounds made it

possible to investigate this question. MIC values of *M. tuberculosis* treated with varying concentrations of INH and either TP2 or TP4 were analyzed using a checkerboard format<sup>32</sup>. Neither synergy nor antagonism were noted when the MIC was used to measure

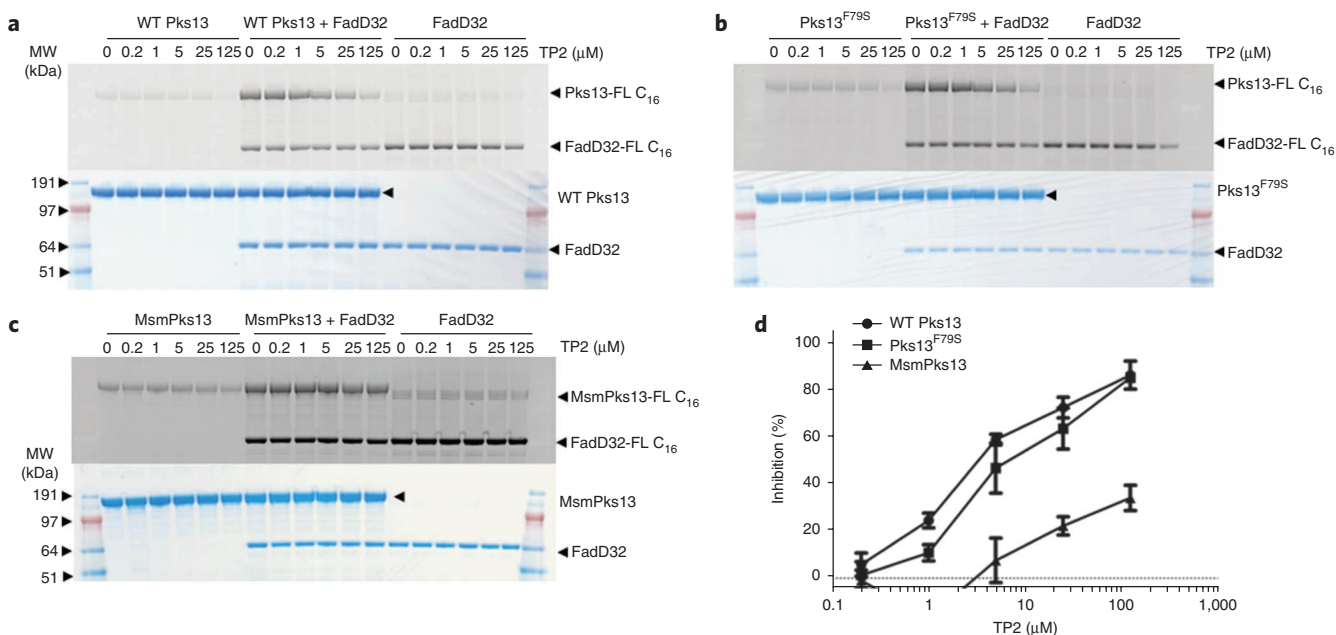


**Figure 2 | Inhibition of fatty acyl-AMP loading onto purified Pks13 by TP2.** (a-d) The loading of FadD32-activated FL C<sub>16</sub> on wild-type (WT) Pks13 (a), Pks13<sup>F79S</sup> (b) and MsmPks13 (c) was determined by separating the reaction mixtures on SDS-PAGE gels. Activities were determined by measuring in-gel fluorescence (top, a-c) and total protein by Coomassie blue staining (bottom, a-c). SeeBlue Plus2 prestained marker (Invitrogen) was used as a molecular weight standard, and approximate molecular weights in MOPS running buffer are indicated. The loading of FL C<sub>16</sub> on wild-type Pks13 (a), Pks13<sup>F79S</sup> (b) and MsmPks13 (c) was quantified using ImageQuant 5.2 (GE healthcare), and the quantification from five replicates (mean ± s.d.) was used to generate the inhibition curve (d). The full-length images corresponding to these figures are shown in **Supplementary Figure 14**.

a combined drug effect (Supplementary Fig. 11). We then determined whether the TP compounds were synergistic with INH for bactericidal activity (as opposed to the bacteriostatic activity reflected in the MIC). For this study, we treated actively growing *M. tuberculosis* cultures with TP2, TP4, INH or RIF alone or with varying combinations of these drugs. Killing was studied in liquid cultures by performing daily measurements of bacterial metabolic activity (growth index) in the BACTEC 460TB system<sup>33,34</sup> (Fig. 3a,b) or by plating for colony-forming units (CFUs) (Fig. 3c). Using metabolic activity measured by the growth index, we found that TP4 killed *M. tuberculosis* at rates similar to those of INH, whereas killing by TP2 was somewhat slower. As measured by CFU viability, TP2 and TP4 killed at slightly slower rates than INH during the initial time points; however, by 7 d, both TP compounds showed better killing than INH. This improved killing persisted for over 20 d (Fig. 3a,c).

The growth index and CFU measurements of INH-treated cultures typically increase after a brief period of decline owing to the rapid emergence of INH-resistant clones<sup>35–39</sup>. The same phenomenon was observed in our study for INH. In contrast, the growth index of cultures treated with the TP2 compounds continued to fall, although viable cells were still detected after 30 d of treatment (Fig. 3a). The CFU of TP-treated cultures also continued to fall for at least 7 d after the CFU of INH-treated cultures began to recover (Fig. 3c). TP-treated cultures did not begin to show an increase in CFU until 20 d after the compounds had been added to the growth medium. Furthermore, whereas approximately half of the regrowth in INH-treated cultures was due to INH-resistant clones (56% resistant to 1  $\mu\text{M}$  of INH or 5 $\times$  the MIC of wild-type INH), only a small fraction of the growth in extensively TP-treated cultures were TP resistant (9.7% TP2 resistant to 5  $\mu\text{M}$  of TP2 or 5 $\times$  the MIC of the wild type; 1.7% TP4 resistant to 2.5  $\mu\text{M}$  of TP4 or 5 $\times$  the MIC of the wild type). RIF caused more rapid and complete killing than the other compounds. Examining the effect of combined treatment, we noted that cultures treated with both INH and a TP compound had initial killing rates that were moderately faster than those of cultures treated with either drug alone (Fig. 3c). Furthermore, the killing curves of the cultures treated with both compounds continued to decrease over time until both growth index and CFU became undetectable (Fig. 3b,c). By the end of the culture period, all of the cells treated with INH plus TP2 or INH plus TP4 seemed to be sterile. Treatment with TP2 or TP4 plus RIF produced killing rates equivalent to that of INH plus RIF. Adding TP2 or TP4 to INH and RIF treatment did not result in further enhancement in killing. However, no antagonism was noted.

### Cytotoxicity and intracellular activity

Several studies were performed to assess the suitability of TP2 or TP4 as potential drug leads. TP2 was shown to have half-maximum inhibitory concentration values versus monkey kidney Vero cells<sup>40</sup> and human liver carcinoma HepG2 cells<sup>41</sup> of 17.5  $\mu\text{M}$  and 7.30  $\mu\text{M}$ , respectively, corresponding to selectivity index values of 17 and 7.3. *M. tuberculosis* is an intracellular pathogen that resides within host macrophages; therefore, we studied the efficiency of TP compounds using a macrophage infection model. Over 90% intracellular killing activity within BCG-infected J774A.1 macrophage cells<sup>40</sup> was observed at TP2 and TP4 concentrations of 12.8  $\mu\text{M}$  and 6.4  $\mu\text{M}$ , respectively, (Supplementary Fig. 12). Overall, these results suggest that these compounds have properties suitable for a drug lead, but additional work will be needed to further increase their potency.

### A possible TP-binding groove on the N-ACP domain of Pks13

To explore the structural basis of Pks13 inhibition by the TP compounds, we performed computational docking<sup>42,43</sup> studies with a comparative model<sup>44</sup> of the Pks13 N-ACP domain (Supplementary Fig. 13a). The vast majority of the lowest free energy binding modes

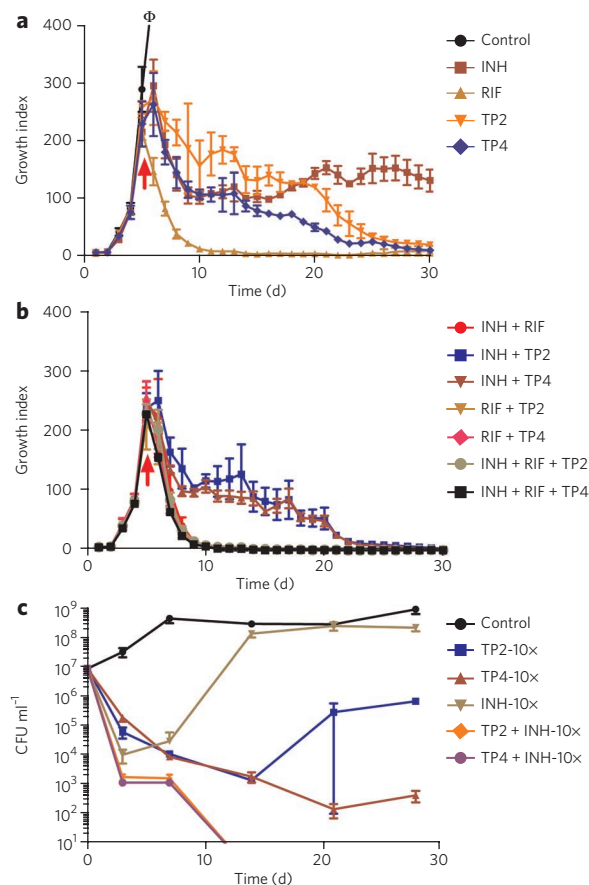


**Figure 3 | Bactericidal activity of TP2, TP4 and other antituberculosis drugs against *M. tuberculosis*.** (a–c) Killing curves of *M. tuberculosis* strain H37Rv after incubation with TP2, TP4, INH, RIF or various combinations of these drugs. Killing activity was monitored using the BACTEC 460TB method at 5 $\times$  the MIC for all of the drug compounds tested either alone (a) or with the indicated drug combinations (b). Killing activity was also monitored by plating for CFU (c) after incubation with the indicated drugs or drug combinations at 10 $\times$  the MIC.  $\phi$  indicates out-of-range growth. The arrows indicate the time when drugs were added to the cultures (in a and b); for c, drugs were added on day zero. The data represented (mean  $\pm$  s.d.) are from two independent experiments performed in triplicates.

for the compounds listed in Table 1 positioned them in a deep, largely neutral and hydrophobic groove separating Ser55 (P-pant site) and Phe79; mutation of Phe79 to serine in DRM2 confers resistance to TP2 and TP4 (Supplementary Fig. 13a). In fact, most of the computationally determined binding modes placed the TP compounds in van der Waals contact with Phe79, which forms the central portion of one face of the TP compound-binding groove. Substituting serine for Phe79 replaces a bulky aromatic hydrophobic side chain with a smaller polar hydrophilic side chain that would alter the hydrophobicity and shape of the TP binding groove by lowering the height of one face (Supplementary Fig. 13b,c). Thus, the results of the docking studies provide a plausible binding site for TP2 and TP4 as well as a reasonable structural explanation for the resistance of the Pks13<sup>F79S</sup> mutant to these compounds.

### DISCUSSION

Here, we demonstrate that the TP compounds inhibit *M. tuberculosis* Pks13, an enzyme involved in a critical step of mycolic acid biosynthesis, establishing it as a vulnerable target for drug development. In this study, (i) we isolated a TP-resistant mutant (DRM2)

with a single SNP, introducing a F79S mutation in Pks13; (ii) computational modeling placed this mutation in close physical proximity to the P-pant attachment site (Ser55) involved in loading of meromycolyl-AMPs by FadD32 (ref. 19), consistent with our findings; (iii) wild-type Pks13 overexpression in *M. tuberculosis* H37Rv led to moderate increases in TP2 MIC, and overexpression of the Pks13<sup>F79S</sup> mutant caused high resistance; (iv) we found that TP2 and TP4 treatment inhibited mycolic acid biosynthesis with the concomitant accumulation of mycolic acid precursors produced by FAS-I in a dose-dependent manner in *M. tuberculosis* H37Rv, whereas discernible mycolic acid inhibition required substantially higher TP concentrations in the TP-resistant DRM2 mutant; and (v) TP compounds effectively inhibit the binding of FadD32-activated FL-C<sub>16</sub> onto Pks13 of TP-susceptible *M. tuberculosis* *in vitro*, but inhibition is diminished in the presence of Pks13 derived from TP-resistant *M. tuberculosis* or from highly TP-resistant *M. smegmatis*.

The identification of Pks13 inhibitors allowed us to explore, for what is to our knowledge the first time, the consequences of Pks13 inhibition in *M. tuberculosis* and to establish Pks13 as a druggable target. We noted that TP4 and INH had almost identical killing curves *in vitro*. Both compounds seemed to leave an unaffected persister population. In the case of INH, study of these persisters has been complicated by the rapid emergence of INH-resistant clones that are either amplified from a pool of pre-existing mutants or generated by INH treatment<sup>35–39</sup>. TP2 and TP4 also generated resistant mutants, albeit to a much lower extent. Our plating studies confirmed that both INH- and TP-treated cultures also contained drug-susceptible persisters. Notably, treatment with a combination of INH and TP compounds not only caused large decreases in cell viability but also seemed to kill persisters, leading to sterilization of the cultures. This is particularly remarkable because it suggests that treatment with two drugs that target different steps in the same metabolic pathway can overcome both persistence and drug resistance that develop in the presence of a single antitubercular agent. We also noted that TP2 was inactive against most nontuberculous mycobacteria. However, this observation is consistent with previous studies showing that several drugs inhibiting mycolic acid biosynthesis in *M. tuberculosis*, including INH or isoxyl, are less active or even totally inactive against *M. smegmatis*<sup>45,46</sup>. TP2 was also inactive against *C. glutamicum* (a strain in which *pks13* is dispensable) and *C. diphtheriae*, further underlining TP2 specificity for Pks13 (Supplementary Table 2).

Although the TP compounds characterized so far have profiles that suggest they are suitable drug leads, their antitubercular activity, intracellular activity and cytotoxicity profile need to be further improved. Our mutation analysis, combined with SAR studies and computational modeling studies, suggests a route for drug optimization. Moreover, our simple and rapid *in vitro* FL C<sub>16</sub> assay, validated with TP2 and TP4, makes it possible to easily screen for other Pks13 inhibitors or TP analogs with improved potency. Complementing this *in vitro* assay, the *in vivo* *piniBAC* induction assay can be used to screen for whole-cell activity.

The F79S TP resistance-producing mutation in the DRM2 strain falls within the Pks13 N-ACP domain near the P-pant site (Ser55), which has been shown to be essential for loading meromycolyl-AMPs by FadD32 (step 2 in Supplementary Fig. 1). We propose that TP2 and TP4 compromise the loading of meromycolyl-AMPs onto the Pks13 N-terminal P-pant site. Our *in vitro* studies showing that TP inhibits FL C<sub>16</sub> loading onto wild-type Pks13 strongly support this hypothesis. The data are also consistent with our computational docking analyses in which the binding groove for TP2 is in between the P-pant site at Ser55 and Phe79. Furthermore, virtually all of the TP compounds that we modeled had a qualitatively better fit for the wild-type protein (Phe79) than the DRM2 mutant (Ser79). Remarkably, the TP binding groove identified in our computational studies was previously proposed to be an acyl chain-binding site

on *Escherichia coli* butyryl-ACP<sup>47</sup> and a P-pant-binding site on *B. subtilis* ACP<sup>48</sup>. It was hypothesized that the acyl chain interaction with the groove could protect the chain during cycles of fatty acid synthesis<sup>47</sup>. We speculate that the P-pant or acyl chain could interact with the Pks13 N-ACP domain and that TP binding could function at least in part to displace the P-pant or acyl chain from the groove, hence affecting Pks13 activity.

This study was enabled by the discovery that certain TP compounds inhibit Pks13. Starting with a series of compounds shown to have bactericidal activity in a whole-cell *M. tuberculosis* screen<sup>25</sup> and taking advantage of the observation that *piniBAC* is induced by a wide variety of compounds that inhibit *M. tuberculosis* cell wall biosynthesis<sup>24</sup>, we developed a relatively unbiased secondary screen for cell wall biosynthesis inhibitors. This approach already led to the discovery of SQ109 and other MmpL3 inhibitors<sup>27,49</sup> as well as the new TP family of compounds reported here. Our discovery of two separate compound classes (DA5 and TP2) that inhibit two distinct steps in mycolic acid biosynthesis (MmpL3 and Pks13, respectively), clearly validates our function-specific promoter screen as a powerful tool for identifying a focused set of drug targets. This promoter will also be useful to characterize modified TP compounds for increased whole-cell activity, given our observed correlation between *piniBAC* activity and TP potency in our preliminary SAR analysis.

In conclusion, we present here a new mechanism for mycolic acid synthesis inhibition that rapidly leads to mycobacterial cell death. Pks13 seems to be a promising target for drugs to treat tuberculosis. The TP inhibitors that are likely to interfere with the function of the N-ACP domain of Pks13 seem to have desirable properties including additive killing and resistance prevention.

Received 12 March 2013; accepted 15 May 2013;  
published online 16 June 2013

## METHODS

Methods and any associated references are available in the [online version of the paper](#).

## References

- Espinal, M.A. The global situation of MDR-TB. *Tuberculosis (Edinb.)* **83**, 44–51 (2003).
- Mondal, R. & Jain, A. Extensively drug-resistant *Mycobacterium tuberculosis*, India. *Emerg. Infect. Dis.* **13**, 1429–1431 (2007).
- Caminero, J.A., Sotgiu, G., Zumla, A. & Migliori, G.B. Best drug treatment for multidrug-resistant and extensively drug-resistant tuberculosis. *Lancet Infect. Dis.* **10**, 621–629 (2010).
- Kroon, A.M. & Van den Bogert, C. Antibacterial drugs and their interference with the biogenesis of mitochondria in animal and human cells. *Pharm. Weekbl. Sci.* **5**, 81–87 (1983).
- Kohanski, M.A., Dwyer, D.J. & Collins, J.J. How antibiotics kill bacteria: from targets to networks. *Nat. Rev. Microbiol.* **8**, 423–435 (2010).
- Wei, J.R. *et al.* Depletion of antibiotic targets has widely varying effects on growth. *Proc. Natl. Acad. Sci. USA* **108**, 4176–4181 (2011).
- Jovetic, S., Zhu, Y., Marcone, G.L., Marinelli, F. & Tramper, J.  $\beta$ -Lactam and glycopeptide antibiotics: first and last line of defense? *Trends Biotechnol.* **28**, 596–604 (2010).
- Khoo, K.H. *et al.* Truncated structural variants of lipoarabinomannan in ethambutol drug-resistant strains of *Mycobacterium smegmatis*. Inhibition of arabinan biosynthesis by ethambutol. *J. Biol. Chem.* **271**, 28682–28690 (1996).
- Vilhéze, C. *et al.* Transfer of a point mutation in *Mycobacterium tuberculosis inhA* resolves the target of isoniazid. *Nat. Med.* **12**, 1027–1029 (2006).
- Slayden, R.A. *et al.* Antimycobacterial action of thiolactomycin: an inhibitor of fatty acid and mycolic acid synthesis. *Antimicrob. Agents Chemother.* **40**, 2813–2819 (1996).
- Glickman, M.S., Cox, J.S. & Jacobs, W.R. Jr. A novel mycolic acid cyclopropane synthetase is required for cording, persistence, and virulence of *Mycobacterium tuberculosis*. *Mol. Cell* **5**, 717–727 (2000).
- Dubnau, E. *et al.* Oxygenated mycolic acids are necessary for virulence of *Mycobacterium tuberculosis* in mice. *Mol. Microbiol.* **36**, 630–637 (2000).
- Bhatt, A., Molle, V., Besra, G.S., Jacobs, W.R. Jr. & Kremer, L. The *Mycobacterium tuberculosis* FAS-II condensing enzymes: their role in mycolic acid biosynthesis, acid-fastness, pathogenesis and in future drug development. *Mol. Microbiol.* **64**, 1442–1454 (2007).

14. Kremer, L., Baulard, A.R. & Besra, G.S. Genetics of mycolic acid biosynthesis. in *Molecular Genetics of Mycobacteria* (eds. Hatfull, G.F. & Jacobs, W.R. Jr.) 173–190 (ASM Press, 2000).
15. Takayama, K., Wang, C. & Besra, G.S. Pathway to synthesis and processing of mycolic acids in *Mycobacterium tuberculosis*. *Clin. Microbiol. Rev.* **18**, 81–101 (2005).
16. Barry, C.E. III *et al.* Mycolic acids: structure, biosynthesis and physiological functions. *Prog. Lipid Res.* **37**, 143–179 (1998).
17. Brennan, P.J. Structure, function, and biogenesis of the cell wall of *Mycobacterium tuberculosis*. *Tuberculosis (Edinb.)* **83**, 91–97 (2003).
18. Ojha, A.K., Trivelli, X., Guerardel, Y., Kremer, L. & Hatfull, G.F. Enzymatic hydrolysis of trehalose dimycolate releases free mycolic acids during mycobacterial growth in biofilms. *J. Biol. Chem.* **285**, 17380–17389 (2010).
19. Gavalda, S. *et al.* The Pks13/FadD32 crosstalk for the biosynthesis of mycolic acids in *Mycobacterium tuberculosis*. *J. Biol. Chem.* **284**, 19255–19264 (2009).
20. Portevin, D. *et al.* A polyketide synthase catalyzes the last condensation step of mycolic acid biosynthesis in mycobacteria and related organisms. *Proc. Natl. Acad. Sci. USA* **101**, 314–319 (2004).
21. Léger, M. *et al.* The dual function of the *Mycobacterium tuberculosis* FadD32 required for mycolic acid biosynthesis. *Chem. Biol.* **16**, 510–519 (2009).
22. Carroll, P., Faray-Kele, M.C. & Parish, T. Identifying vulnerable pathways in *Mycobacterium tuberculosis* by using a knockdown approach. *Appl. Environ. Microbiol.* **77**, 5040–5043 (2011).
23. Sasseti, C.M. & Rubin, E.J. Genetic requirements for mycobacterial survival during infection. *Proc. Natl. Acad. Sci. USA* **100**, 12989–12994 (2003).
24. Alland, D., Steyn, A.J., Weisbrod, T., Aldrich, K. & Jacobs, W.R. Jr. Characterization of the *Mycobacterium tuberculosis* *iniBAC* promoter, a promoter that responds to cell wall biosynthesis inhibition. *J. Bacteriol.* **182**, 1802–1811 (2000).
25. Maddry, J.A. *et al.* Antituberculosis activity of the molecular libraries screening center network library. *Tuberculosis (Edinb.)* **89**, 354–363 (2009).
26. Ananthan, S. *et al.* High-throughput screening for inhibitors of *Mycobacterium tuberculosis* H37Rv. *Tuberculosis (Edinb.)* **89**, 334–353 (2009).
27. Tahlan, K. *et al.* SQ109 targets MmpL3, a membrane transporter of trehalose monomycolate involved in mycolic acid donation to the cell wall core of *Mycobacterium tuberculosis*. *Antimicrob. Agents Chemother.* **56**, 1797–1809 (2012).
28. Telenti, A. *et al.* The *emb* operon, a gene cluster of *Mycobacterium tuberculosis* involved in resistance to ethambutol. *Nat. Med.* **3**, 567–570 (1997).
29. Onodera, Y., Tanaka, M. & Sato, K. Inhibitory activity of quinolones against DNA gyrase of *Mycobacterium tuberculosis*. *J. Antimicrob. Chemother.* **47**, 447–450 (2001).
30. Trivedi, O.A. *et al.* Enzymic activation and transfer of fatty acids as acyl-adenylates in mycobacteria. *Nature* **428**, 441–445 (2004).
31. Freundlich, J.S. *et al.* Triclosan derivatives: towards potent inhibitors of drug-sensitive and drug-resistant *Mycobacterium tuberculosis*. *ChemMedChem* **4**, 241–248 (2009).
32. Reddy, V.M., Einck, L., Andries, K. & Nacy, C.A. *In vitro* interactions between new antitubercular drug candidates SQ109 and TMC207. *Antimicrob. Agents Chemother.* **54**, 2840–2846 (2010).
33. Siddiqi, S.H., Libonati, J.P. & Middlebrook, G. Evaluation of rapid radiometric method for drug susceptibility testing of *Mycobacterium tuberculosis*. *J. Clin. Microbiol.* **13**, 908–912 (1981).
34. Safi, H., Sayers, B., Hazbon, M.H. & Alland, D. Transfer of *embB* codon 306 mutations into clinical *Mycobacterium tuberculosis* strains alters susceptibility to ethambutol, isoniazid, and rifampin. *Antimicrob. Agents Chemother.* **52**, 2027–2034 (2008).
35. Middlebrook, G. Sterilization of tubercle bacilli by isonicotinic acid hydrazide and the incidence of variants resistant to the drug *in vitro*. *Am. Rev. Tuberc.* **65**, 765–767 (1952).
36. Siddiqi, S., Takhar, P., Baldeviano, C., Glover, W. & Zhang, Y. Isoniazid induces its own resistance in nonreplicating *Mycobacterium tuberculosis*. *Antimicrob. Agents Chemother.* **51**, 2100–2104 (2007).
37. Gumbo, T. *et al.* Isoniazid bactericidal activity and resistance emergence: integrating pharmacodynamics and pharmacogenomics to predict efficacy in different ethnic populations. *Antimicrob. Agents Chemother.* **51**, 2329–2336 (2007).
38. Gumbo, T. *et al.* Isoniazid's bactericidal activity ceases because of the emergence of resistance, not depletion of *Mycobacterium tuberculosis* in the log phase of growth. *J. Infect. Dis.* **195**, 194–201 (2007).
39. Wallis, R.S. *et al.* Drug tolerance in *Mycobacterium tuberculosis*. *Antimicrob. Agents Chemother.* **43**, 2600–2606 (1999).
40. Falzari, K. *et al.* *In vitro* and *in vivo* activities of macrolide derivatives against *Mycobacterium tuberculosis*. *Antimicrob. Agents Chemother.* **49**, 1447–1454 (2005).
41. Boechat, N. *et al.* Novel 1,2,3-triazole derivatives for use against *Mycobacterium tuberculosis* H37Rv (ATCC 27294) strain. *J. Med. Chem.* **54**, 5988–5999 (2011).
42. Morris, G.M. *et al.* AutoDock4 and AutoDockTools4: automated docking with selective receptor flexibility. *J. Comput. Chem.* **30**, 2785–2791 (2009).
43. Trott, O. & Olson, A.J. AutoDock Vina: improving the speed and accuracy of docking with a new scoring function, efficient optimization, and multithreading. *J. Comput. Chem.* **31**, 455–461 (2010).
44. Sali, A. & Blundell, T.L. Comparative protein modelling by satisfaction of spatial restraints. *J. Mol. Biol.* **234**, 779–815 (1993).
45. Phetsuksiri, B. *et al.* Antimycobacterial activities of isoxyl and new derivatives through the inhibition of mycolic acid synthesis. *Antimicrob. Agents Chemother.* **43**, 1042–1051 (1999).
46. Kremer, L. *et al.* Inhibition of InhA activity, but not KasA activity, induces formation of a KasA-containing complex in mycobacteria. *J. Biol. Chem.* **278**, 20547–20554 (2003).
47. Roujeinikova, A. *et al.* X-ray crystallographic studies on butyryl-ACP reveal flexibility of the structure around a putative acyl chain binding site. *Structure* **10**, 825–835 (2002).
48. Parris, K.D. *et al.* Crystal structures of substrate binding to *Bacillus subtilis* holo-(acyl carrier protein) synthase reveal a novel trimeric arrangement of molecules resulting in three active sites. *Structure* **8**, 883–895 (2000).
49. Lee, R.E. *et al.* Combinatorial lead optimization of [1,2]-diamines based on ethambutol as potential antituberculosis preclinical candidates. *J. Comb. Chem.* **5**, 172–187 (2003).

## Acknowledgments

This work was supported in part by US National Institutes of Health (NIH) grant R01 AI080653 to D.A., a United Negro College Fund–Merck Postdoctoral Science Research Fellowship to R.W., a grant from the University of Medicine and Dentistry of New Jersey (UMDNJ) foundation to R.C. and NIH grant R01 AI081736 to M.B.N. W.R.J. acknowledges generous support from the NIH Centers for AIDS research grant AI-051519 at the Albert Einstein College of Medicine and by NIH grant AI26170. The compounds initially screened in this work were supplied as part of NIH grants AI-95364 and AI-15449. We thank R.C. Goldman (formally Department of Health and Human Services, NIH, and Division of Microbiology and Infectious Diseases, National Institute of Allergy and Infectious Diseases (NIAID), currently RCG Consulting) for his support obtaining Molecular Libraries Probe Centers Network (MLPCN) compounds for the *piniBAC* screen, R. Reynolds (Southern Research Institute) for his advice on the initial analysis of the MLPCN library and C.E. Barry, III and H.I.M. Boshoff (Tuberculosis Research Section, Laboratory of Clinical Infectious Diseases, NIAID, NIH) for their kind gift of TDM and TMM standards. The MS data were obtained from an Orbitrap instrument funded in part by NIH grant NS046593 for the support of the UMDNJ Neuroproteomics Core Facility.

## Author contributions

R.W., P.K., C.V., W.R.J., L.K. and D.A. conceived and designed experiments. J.S.F. synthesized compound JSF-1735, and M.J.S. and J.S.F. synthesized FAME standards. V.P. and M.B.N. performed computational docking studies. S.W.B. and J.R.W. performed whole-genome sequencing and analysis. R.W., P.K., C.V., R.V.-C., E.M., S.S., R.C. and L.K. performed whole-cell screening; performed MIC testing; selected resistant mutants; constructed recombinant strains; performed mycolic acid analyses; overexpression studies; and bactericidal, intracellular and synergy assays. R.W., P.K. and D.A. wrote the manuscript. All of the authors discussed the results and commented and contributed to sections of the manuscript.

## Competing financial interests

The authors declare no competing financial interests.

## Additional information

Supplementary information, chemical compound information and chemical probe information are available in the [online version of the paper](#). Reprints and permissions information is available online at <http://www.nature.com/reprints/index.html>. Correspondence and requests for materials should be addressed to D.A.

## ONLINE METHODS

**Bacterial strains, culture conditions, primers and plasmids.** *M. tuberculosis* strains were obtained from laboratory stocks. Clinical strains were obtained from a collection of clinical isolates established by UNICEF, UNDP, World Bank and WHO Special Programs for Research and Training in Tropical Diseases (TDR). All of the *M. tuberculosis* strains were grown at 37 °C in Middlebrook medium 7H9 (Becton Dickinson, Sparks, MD) enriched with 10% oleic acid-albumin-dextrose-catalase (OADC-Becton Dickinson) and 0.05% (w/v) Tween-80 or Tyloxapol in liquid medium. Middlebrook 7H10 agar (Becton Dickinson) supplemented with 10% OADC and 0.5% glycerol (v/v) was used to grow strains on solid medium.

**Reporter screen for cell wall biosynthesis inhibitors.** A total of 1,113 compounds previously identified as having antitubercular activity in a whole-cell screen of a 100,997 compound library<sup>25,26</sup> (performed at the Southern Research Institute for the MLPCN and the Tuberculosis Antimicrobial Acquisition and Coordinating Facility program under NIH contracts N01-AI-95364 and N01-AI 15449)<sup>25</sup> were tested for their ability to induce the *iniBAC* promoter (*piniBAC*). The promoter screen used a BCG strain (BCG<sup>s</sup>(pG4697-6)) containing the *iniBAC* promoter sequence fused to a *lacZ* reporter (pG4697-6)<sup>24</sup>. The BCG<sup>s</sup>(pG4697-6) was grown to an  $D_{600\text{ nm}}$  of 0.6, and 90  $\mu\text{l}$  was dispensed into each well of 96-well plates, then 10  $\mu\text{l}$  of each compound (final concentration  $1 \times \text{IC}_{90}$ ) was added. After incubation for 24 h at 37 °C, 100  $\mu\text{l}$  of LacZ buffer (60 mM Na<sub>2</sub>HPO<sub>4</sub>·7H<sub>2</sub>O, 40 mM NaH<sub>2</sub>PO<sub>4</sub>·H<sub>2</sub>O, 10 mM KCl, 1 mM MgSO<sub>4</sub>·7H<sub>2</sub>O, 50 mM  $\beta$ -mercaptoethanol), 5  $\mu\text{l}$  of chloroform and 2  $\mu\text{l}$  of 0.1% SDS were added and incubated for 5 min at room temperature (RT). Then, 40  $\mu\text{l}$  of 4 mg/ml of 2-nitrophenyl  $\beta$ -D-galactopyranoside (Sigma Aldrich, St. Louis, MO) was added to each well, and plates were incubated for 15 min. Following incubation, 100  $\mu\text{l}$  of 1 M sodium carbonate was added to each well, and absorbance was read at 420 nm. Fold induction was determined by the  $D_{420\text{ nm}}$  of the wells treated with compounds/ $D_{420\text{ nm}}$  of the wells to which compounds were not added (Table 1 and Supplementary Table 1). EMB and INH were used as positive induction controls.

**Construction of overexpression strains.** For the overexpression of Pks13 variants in mycobacteria, we used pVV16 (ref. 50), pMK1 (ref. 51) and pMV306-Hyg<sup>52</sup> vectors. All of the primer sequences and plasmids used in this study are given in Supplementary Tables 4 and 5, respectively.

**MIC, synergy and bactericidal activity assays.** MIC values were determined using the standard radiometric BACTEC 460TB method (Becton Dickinson)<sup>33,34</sup>. Antibiotics were purchased from Sigma Aldrich, and thiophene analogs (Table 1) were purchased by Chembridge except for TP1735 that was synthesized as described below. Compounds were stored as stocks at 20 mg/ml in DMSO. For the BACTEC-based bactericidal activity assays, each vial of 12B medium was inoculated with H37Rv at  $2 \times 10^5$  CFU and grown to a growth index of 200. Test drugs were then added to these vials either singly or in combination. The bottles were incubated at 37 °C, and then the growth index of each bottle was measured daily. Drug concentrations used for the bactericidal studies were calculated to be approximately 5 $\times$  the MIC for INH (1.1  $\mu\text{M}$ ), RIF (1.2  $\mu\text{M}$ ), TP2 (5.0  $\mu\text{M}$ ) and TP4 (2.5  $\mu\text{M}$ ), except where noted. The MIC assays in 96-well format were performed using the microdilution method<sup>53</sup>.

**Synthesis of TP1735.** Methyl ester (10 mg, 0.0237 mmol) was dissolved in 1.0 ml dioxane and subjected to the addition of aqueous lithium hydroxide (2.0 M solution, 5.0 equiv., 0.118 mmol, 60  $\mu\text{l}$ ). The brown, slightly turbid solution was stirred for 2 h at RT and then for 2 d at 40 °C. At this point, TLC analysis demonstrated consumption of starting material. The basic solution was washed with 3  $\times$  5 ml diethyl ether, acidified to  $\sim$ pH 1 with 1 N HCl<sub>(aq)</sub> and extracted with 3  $\times$  5 ml ethyl acetate. The organics were washed with 5 ml saturated aqueous brine solution, dried over anhydrous magnesium sulfate for 5 min and concentrated by vacuum to produce 8 mg of white solid. Recrystallization of this crude product from acetone at 0 °C produced analytically pure white crystals in the amount of 3 mg (0.00761 mmol, 33%). <sup>1</sup>H NMR (400 MHz, d<sub>4</sub>-MeOH)  $\delta$ 12.4 (br s, 1), 6.92 (br s, 2), 2.76 (s, 3); <sup>19</sup>F NMR (376 MHz, d<sub>4</sub>-MeOH)  $\delta$ -141.8, -151.8, -162.8; LC-MS (ES<sup>+</sup>) - 1.73 min (96% purity @ 215 nm); HRMS: 394.0067 Da; found; expected 394.0067 Da. NMR experiments were performed on a Bruker Avance 400 MHz NMR spectrometer. Low-resolution LC/MS experiments were achieved with a Shimadzu 2010 LC/MS instrument equipped with an electrospray source. High-resolution MS

(HR MS) data were performed on an Agilent Technologies 6210 series TOF mass spectrometer coupled to an Agilent Technologies 1200 series HPLC system using no HPLC column.

**Isolation of DRM2 and whole-genome sequencing.** The TP2-resistant *M. tuberculosis* mutant, DRM2, was isolated by plating ten-fold serial dilutions of liquid cultures at  $D_{600\text{ nm}} \sim 1.5$  onto 7H10 plates containing 3.8  $\mu\text{M}$  and 7.6  $\mu\text{M}$  of TP2. Plates were screened for resistant colonies after 3–6 weeks at 37 °C. The genomic DNA was isolated<sup>54</sup> from DRM2 and subjected to whole-genome sequencing and single nucleotide polymorphism (SNP) analysis<sup>27</sup>.

**Analysis of mycolic acids and other lipids.** For the analysis of MAMES and FAMES<sup>55</sup>, the compounds were added to 4 ml of *M. tuberculosis* cultures ( $D_{600\text{ nm}}$  of  $\sim 1.5$ ), incubated at 37 °C for 15 h, and 1  $\mu\text{Ci/ml}$  of [<sup>14</sup>C]acetate (56 mCi/mmol) was added to each culture. Following incubation at 37 °C for another 8 h, the [<sup>14</sup>C]-labeled cells were harvested, washed with PBS and sterilized by autoclaving. The lipids from cell pellets were hydrolyzed by adding 2 ml of tetra-*n*-butylammonium hydroxide (TBAH) by incubating overnight at 100 °C. Fatty acids were esterified by adding 4 ml CH<sub>2</sub>Cl<sub>2</sub>, 300  $\mu\text{l}$  CH<sub>3</sub>I and 2 ml distilled water (dH<sub>2</sub>O) and mixing at RT for 1 h. After centrifugation, the upper phase was discarded, and samples were washed twice with dH<sub>2</sub>O. The lower phase was dried and resuspended in 3 ml of diethylether, and after centrifugation the organic phase was dried, and lipids were resuspended in 200  $\mu\text{l}$  CH<sub>2</sub>Cl<sub>2</sub>. Equal counts (75,000 c.p.m.) were loaded on a silica gel 60 F254 thin-layer chromatography (TLC) plate and resolved using hexane/ethyl acetate (19:1, v/v, 2 runs). The FAMES and MAMES were detected by autoradiography. To determine the chain-length distribution of FAMES, the *M. tuberculosis* cultures (4 ml each at  $D_{600\text{ nm}}$  of 0.3) were treated with compounds for 2 h, followed by [<sup>14</sup>C]acetate incorporation for another 2 h, and then MAMES and FAMES were prepared as above. The samples (5  $\mu\text{l}$  each) were analyzed on a C<sub>18</sub> reverse-phase TLC, developed with acetonitrile/dioxane (1:1, v/v) and analyzed by phosphorimaging. To study the effect of compounds on polar lipids including TMM and TDM, labeled cell pellets were extracted overnight at 50 °C with 4 ml of CHCl<sub>3</sub> in CH<sub>3</sub>OH (2:1, v/v)<sup>27</sup>. After centrifugation, the supernatants were dried and dissolved in 200  $\mu\text{l}$  CHCl<sub>3</sub> in CH<sub>3</sub>OH (2:1). An equal volume (5  $\mu\text{l}$ ) of each sample was analyzed on normal phase TLC plates and developed with CHCl<sub>3</sub>/CH<sub>3</sub>OH/H<sub>2</sub>O (62:25:4, v/v/v). For the analysis of apolar lipids, *M. tuberculosis* cultures 10 ml each ( $D_{600\text{ nm}}$  of  $\sim 1.0$ )<sup>56</sup> were treated with TP2 or orlistat (Sigma Aldrich) for 6 h followed by 5  $\mu\text{Ci}$  [<sup>14</sup>C]propionate (American Radiolabeled Chemicals, Inc., St. Louis, MO). After incubation for 16 h at 37 °C, the cell pellets were extracted with 2 ml CH<sub>3</sub>OH/0.3% NaCl (10:1) and 1 ml petroleum ether by vigorously mixing over 15 min. After centrifugation, the upper layer was dried, resuspended in 200  $\mu\text{l}$  of petroleum ether, spotted (5  $\mu\text{l}$  each) on normal-phase TLC plates and developed either with CHCl<sub>3</sub>/CH<sub>3</sub>OH/H<sub>2</sub>O (62:12:1, v/v/v) or petroleum ether/ethyl acetate (98:2, v/v, three times)<sup>57,58</sup>. The TLCs were visualized using a phosphorimager.

**Synthesis of FAMES for RP-TLC analysis.** One millimole of each fatty acid was dissolved or suspended in 4 ml of 50% ethyl ether/methanol at RT. Trimethylsilyldiazomethane (2 M in hexanes, Sigma Aldrich) was added at a rate such that insoluble acids dissolved and the rate of gas evolution was controlled. When a yellow color persisted, the mixture was aged for 1 h. The reaction was quenched by the dropwise addition of glacial acetic acid until the solution was colorless. The solution was then partitioned between ethyl ether and saturated aq. sodium bicarbonate. The organic layer was decanted, washed with brine, dried over magnesium sulfate, concentrated and purified via flash chromatography with a 4 g silica cartridge (RedisSep) on an Isco Combiflash Companion using a 1–>5% ethyl acetate–hexanes gradient. Fractions containing product were identified using silica gel 60 TLC plates eluted with 10% ethyl ether–hexanes and visualized by dipping in a solution of 10% phosphomolybdic acid in isopropanol and heating on a hot plate. Analyzed on an Agilent LC/MS, the products were not detectable by UV in positive or negative ion mode. All gave satisfactory NMR spectra.

**Fadd32 dependent loading of BODIPY FL C<sub>16</sub> in Pks13.** The loading assay of the N-term ACP domain was adapted from previous study<sup>19</sup>. The [<sup>14</sup>C]palmitic acid (C<sub>16</sub>) substrate was substituted with fluorescein-labeled palmitic acid. The Pks13 protein was incubated with 50  $\mu\text{M}$  BODIPY FL C<sub>16</sub> (Invitrogen, D-3821) in 1 $\times$  Pks13 reaction buffer (50 mM HEPES, pH 7.2, 7 mM trehalose, 7 mM glucose, 2 mM ATP, 8 mM MgCl<sub>2</sub>) at 30 °C with and without Fadd32 (1  $\mu\text{M}$ ) in

20- $\mu$ l reactions. After 2-h incubations, the reactions were terminated by adding 5  $\mu$ l of 6 $\times$  Laemmli sample buffer and quantified as described below.

**Inhibition of BODIPY FL C<sub>16</sub> incorporation in Pks13 by TP2 and TP4.** The Pks13 protein (1.0  $\mu$ M) was preincubated with indicated (Fig. 2 and Supplementary Fig. 9) amounts of TP compounds at RT and ice for 15 min each in 10  $\mu$ l (25 mM Tris, pH 8.0, 25 mM NaCl). The reactions were initiated by adding 10  $\mu$ l of 2 $\times$  Pks13 reaction mixture containing 100  $\mu$ M FL C<sub>16</sub> and incubated at 30 °C for 2 h. The reactions were terminated by adding Laemmli sample buffer (100 °C for 5 min) and separated on 4–12% NuPAGE novex Bis-Tris gel (Invitrogen) using 1 $\times$  MOPS running buffer. After electrophoresis, the in-gel fluorescence was measured using Typhoon 9400. The total amount of protein in the gels was visualized with InstantBlue stain (Expediton Inc., San Diego, CA). The fluorescence was quantified (RFU or relative fluorescence units) using ImageQuant software. For quantitative analysis, a common background correction was applied to all spots, and the activity was determined by subtracting counts corresponding to Pks13 only and FadD32 only from counts of both enzymes used together ( $\text{Activity}_{\text{RFU}} = \text{RFU}_{(\text{Pks13} + \text{FadD32})} - \text{RFU}_{(\text{Pks13})} - \text{RFU}_{(\text{FadD32})}$ ). The percentage inhibition was calculated considering no inhibitor control as 100% activity (inhibition % =  $1 - (100 \times (\text{Activity}_{\text{RFU}} \text{ in the presence of inhibitor} / \text{Activity}_{\text{RFU}} \text{ in the absence of inhibitor}))$ ).

**Purification of *M. tuberculosis* and *M. smegmatis* Pks13 in *E. coli*.** The *E. coli* expression constructs in pET26b vector were cotransformed with pLysS-*sfp* into *E. coli* BL21 (DE3). The purification was carried out as described previously<sup>19</sup> using affinity (Talon resin, as detailed below for FadD32) and gel filtration (Superdex-200, GE Healthcare) chromatography.

**Confirmation of P-pant modification in peptide containing Ser55.** The P-pant status of *M. tuberculosis* Pks13 at S55 was confirmed by trypsin digestion and nano-LC/MS/MS (Supplementary Fig. 3) as described previously<sup>19</sup>. Briefly, 5  $\mu$ g Pks13 was precipitated with TCA digested with trypsin, peptides were desalted using C<sub>18</sub> spin columns, and capillary-LC-nanospray tandem MS (nano-LC/MS/MS) was performed on a Thermo Finnigan LTQ orbitrap velos mass spectrometer equipped with a nanospray source operated in positive ion mode. The LC system was an UltiMate 3000 (Dionex, Sunnyvale, CA) with a FAMOS autosampler. Solvent A contained 2% acetonitrile and 0.1% formic acid. Solvent B contained 95.0% acetonitrile and 0.1% formic acid. Five microliters of each sample was injected onto a reversed phase 0.3 mm  $\times$  5 mm trapping column (LC-Packings A Dionex Co, Sunnyvale, CA) and washed with solvent A. The injector port was switched to inject, and the peptides were eluted off of the trap and resolved on a 75  $\mu$ m  $\times$  150 mm capillary PepMap column (3  $\mu$ m, 100 Å, C<sub>18</sub>, Dionex). Peptides were eluted into the LTQ system using a gradient of 10–95% B over 60 min, with a flow rate of 250 nl/min. The scan sequence of the mass spectrometer was programmed to perform a full scan followed by ten data-dependent MS/MS scans of the most abundant peaks in the spectrum. Dynamic exclusion was used to exclude multiple MS/MS of the same peptide. Data were searched against the Pks13 sequence along with contaminants on the mascot search engine with the following parameters: trypsin as a protease, one missed cleavage, P-pant as variable modification. Precursor ion tolerance was set at 10 p.p.m., and fragment ion tolerance was set at 0.5 Da. Matched spectra were manually verified for confirmation.

**Purification and activity of *M. tuberculosis* FadD32.** The pET26b-*fadD32* was transformed into *E. coli* BL21(DE3) and grown in 500 ml autoinduction medium (Overnight Express Autoinduction System 1, Novagen) supplemented with kanamycin (50  $\mu$ g/ml) at 18 °C for 72 h. The cells were harvested and resuspended in 40 ml of lysis buffer (50 mM Tris-HCl, pH 8.0, 300 mM NaCl, 10 mM imidazole, 0.1% Triton-X100, 1 mg/ml lysozyme, 1 $\times$  EDTA free-protease inhibitor cocktail) and frozen overnight at -80 °C. The cells were lysed by sonication, and the clarified supernatant was allowed to bind with 2 ml Talon resin (Clontech) at 4 °C for 1 h. The resin was washed in 3  $\times$  30 ml wash buffer (50 mM Tris-HCl, pH 8.0, 300 mM NaCl, 10 mM imidazole), eluted with 15 ml elution buffer (50 mM Tris-HCl, pH 8.0, 50 mM NaCl, 500 mM imidazole), concentrated by an Amicon centrifugal device, washed with 50 ml of 50 mM Tris-HCl, pH 8.0, with 50 mM NaCl and dialyzed overnight in storage buffer (50 mM Tris-HCl, pH 8.0, 50 mM NaCl, 50% glycerol). The activity and inhibition of FadD32 by TP2 and TP4 was determined using a radioTLC assay<sup>30</sup> performed under same the conditions as Pks13 assays. The FadD32 (1  $\mu$ M for TP2 and 2  $\mu$ M for TP4) was preincubated with the indicated amount

of TP compound at RT followed by incubation on ice for 15 min each. The reactions were initiated by adding [<sup>14</sup>C]lauric acid (50  $\mu$ M) as substrate in 1 $\times$  reaction buffer and terminated by adding glacial acetic acid (final concentration 2%). Fractions of the reactions (2.5  $\mu$ l) were analyzed on silica gel G-60 TLC plates in n-butanol/acetic acid/water (80:25:40, v/v/v) solvent system and visualized by phosphorimaging.

**Determination of drug interactions (synergism and antagonism).** *M. tuberculosis* H37Rv was treated with two-fold serial dilutions of INH and TP2 or INH and TP4 or either drug alone with concentrations ranging from 0.05–0.40  $\mu$ M and 0.125–1  $\mu$ M, respectively. Growth was monitored using the Bactec 460TB method<sup>33,34</sup>. Compound concentrations that inhibited growth compared to the compound-free 12B medium 1:100 dilution control were defined as negative (-) for growth. A checkerboard analysis<sup>32</sup> was used to determine synergy and antagonism of the TP compounds with INH. The fractional inhibitory concentration (FIC) was determined by dividing the MIC of the combination of drugs by the MIC of the drugs independently. The fractional inhibitory index ( $\Sigma$ FIC) was determined by adding the FIC values of each drug tested. The activity of compounds was defined as synergistic if  $\Sigma$ FIC  $\leq$  0.5, antagonistic if  $\Sigma$ FIC  $\geq$  4.0 and independent if  $\Sigma$ FIC  $>$  0.5 and  $<$  4.0 (ref. 32).

**Killing studies using CFU measurements.** For the CFU-based bactericidal activity assays, H37Rv was grown in Middlebrook 7H9-OADC-tyloxapol-glycerol to mid-log phase ( $D_{600 \text{ nm}}$  of  $\sim$ 1.0). The cultures were diluted 1:50 and incubated with TP compounds at 37 °C while stirring. At specific time points, aliquots were taken, and serial dilutions were plated on Middlebrook 7H10-OADC-glycerol. The plates were incubated at 37 °C for 4 weeks, and CFUs were counted.

**Measuring the emergence of drug resistance during BACTEC killing studies.** To determine the proportion of resistant cells that emerged upon prolonged drug treatment, bacterial cells were removed from their BACTEC vials after 48 d of drug treatment, spun down and serially diluted for CFU determination onto 7H10 plates containing varying concentrations of the relevant drug.

**Cytotoxicity assays.** Cytotoxicity studies were performed by a commercial vendor (Pharmaron Inc.). In brief, Vero (African green monkey kidney epithelial) and HepG2 (human liver carcinoma) cells were grown to exponential growth phase and seeded on 96-well microplates at a final concentration of  $5 \times 10^4$  cells/ml in medium containing 10% FBS. Three-fold serial dilutions of TP2 with a starting concentration of 20 mM were added to wells, and plates were incubated for 72 h in a 37 °C, 5% CO<sub>2</sub> incubator. After incubation, 150  $\mu$ l XTT solution (0.33 mg XTT/ml free phenol red RPMI 1640 medium) was added per well, and plates were incubated for an additional 2 h in a CO<sub>2</sub> incubator (5%, 37 °C). Following incubation, plates were shaken for 5 min at 200 r.p.m., and absorbance was read at 450 nm. Paclitaxel, a mitotic inhibitor, was used as a positive control.

**Intracellular activity in J774A.1 murine macrophages.** J774A.1 macrophages were seeded onto 24-well clear plates at  $1 \times 10^5$  cells/well, incubated at 37 °C for 16 h and infected with BCG at an MOI of 5. After incubation at 37 °C for 1 h, cells were treated with amikacin (200  $\mu$ g/ml) for 2 h. The cells were washed 3 $\times$  with Hank's Balanced Saline Solution (HBSS) and incubated at 37 °C for  $\sim$ 16 h. After incubation, compounds were added. On day 6, cells were washed with 3 $\times$  HBSS to remove excess compounds, lysed with dH<sub>2</sub>O, serially diluted and plated on 7H10 medium for CFU.

**Comparative modeling and thiophene compound docking.** Comparative models of the wild-type and F79S mutant Pks13 N-ACP domain were generated using MODELLER<sup>44</sup>. The high-resolution X-ray crystal structure of an acyl carrier protein (Protein Data Bank code 1X3O) from *Thermus thermophilus* was used as the modeling template. The Pks13 N-ACP domain model (residues 18–95) yielding the lowest DOPE score and a GA341 score of 0.99975 was selected for the thiophene compound docking studies. AutoDock Tools<sup>42</sup> was used to prepare the thiophene compound models and the Pks13 N-ACP domain model for docking in AutoDock Vina<sup>43</sup>. The docking grid encompassed the entire Pks13 N-terminal ACP domain, and no residues were selected as flexible. Molecular graphics were produced with PyMOL<sup>59</sup>.

50. Jackson, M., Crick, D.C. & Brennan, P.J. Phosphatidylinositol is an essential phospholipid of mycobacteria. *J. Biol. Chem.* **275**, 30092–30099 (2000).

51. Veyron-Churlet, R., Zanella-Cleon, I., Cohen-Gonsaud, M., Molle, V. & Kremer, L. Phosphorylation of the *Mycobacterium tuberculosis*  $\beta$ -ketoacyl-acyl carrier protein reductase MabA regulates mycolic acid biosynthesis. *J. Biol. Chem.* **285**, 12714–12725 (2010).
52. Stover, C.K. *et al.* New use of BCG for recombinant vaccines. *Nature* **351**, 456–460 (1991).
53. Kim, P. *et al.* Structure-activity relationships of antitubercular nitroimidazoles. 2. Determinants of aerobic activity and quantitative structure-activity relationships. *J. Med. Chem.* **52**, 1329–1344 (2009).
54. van Soolingen, D., Hermans, P.W., de Haas, P.E., Soll, D.R. & van Embden, J.D. Occurrence and stability of insertion sequences in *Mycobacterium tuberculosis* complex strains: evaluation of an insertion sequence-dependent DNA polymorphism as a tool in the epidemiology of tuberculosis. *J. Clin. Microbiol.* **29**, 2578–2586 (1991).
55. Slayden, R.A. & Barry, C.E. III. Analysis of the lipids of *Mycobacterium tuberculosis*. *Methods Mol. Med.* **54**, 229–245 (2001).
56. Seeliger, J.C. *et al.* Elucidation and chemical modulation of sulfolipid-1 biosynthesis in *Mycobacterium tuberculosis*. *J. Biol. Chem.* **287**, 7990–8000 (2012).
57. Domenech, P. & Reed, M.B. Rapid and spontaneous loss of phthiocerol dimycocerosate (PDIM) from *Mycobacterium tuberculosis* grown *in vitro*: implications for virulence studies. *Microbiology* **155**, 3532–3543 (2009).
58. Alibaud, L. *et al.* A *Mycobacterium marinum* TesA mutant defective for major cell wall-associated lipids is highly attenuated in *Dictyostelium discoideum* and zebrafish embryos. *Mol. Microbiol.* **80**, 919–934 (2011).
59. DeLano, W.L. *The PyMOL Molecular Graphics System* (DeLano Scientific, San Carlos, California, USA, 2002).